Eng. Sci., 2021, **17**, 224–230

Engineered Science
DOI: https://dx.doi.org/10.30919/es8e509

Optical Properties of a Core/Shell/Shell Shape Metal-Insulator-Metal Composite Nanoparticle for Solar Energy Absorption

Caiyan Qin,[1] Han Gong,[2] Chunlei Sun[3] and Xiaohu Wu[4,*]

Abstract

Due to their excellent photothermal properties, plasmonic nanofluids have been intensively studied in the field of solar thermal utilization. Metallic nanoparticles, such as Au and Ag, of different shapes have been widely investigated taking advantage of the localized surface plasmon resonance (LSPR) effect. However, the nanoparticles which can excite magnetic resonance apart from the LSPR effect have been rarely studied. In this study, a core/shell/shell shape Ag-SiO_2-Ag composite nanoparticle has been proposed for exciting both magnetic resonance and LSPR, giving rise to multiple absorption peaks and broadband absorption. The resonance modes have also been investigated by analyzing the local electromagnetic field. In addition, the effects of size parameters and material of the nanoparticles on the optical properties have been studied to explore the possibility to broaden the absorption peaks. The findings in this work suggest that the core/shell/shell shape metal-insulator-metal composite nanoparticles can be promising candidates for solar thermal harvest.

Keywords: Solar thermal; Composite nanoparticles; Magnetic resonances; Localized surface plasmon resonance.
Received: 01 July 2021; Revised: 03 August 2021; Accepted: 10 August 2021.
Article type: Research article.

1. Introduction

With the world's fast economic development, the demand for energy increases year by year, and the consumption of fossil energy especially intensifies. Under such circumstances, the development of renewable energy is of great significance. Due to the advantages of wide distribution, large reserves, and environmental friendliness, solar energy as an important renewable energy source has attracted more and more attention from researchers.[1] The use of solar energy mainly includes photothermal conversion, photoelectric conversion, and photochemical conversion.[2] Photoelectric conversion refers to the utilization of solar energy via photovoltaic cells. The active band of the photovoltaic materials, usually silicon, limits its effectiveness. Photochemical conversion mainly refers to solar energy-fueled hydrogen production, which is still in the preliminary research stage. In comparison, photothermal can utilize the full solar spectrum, converting all the absorbed solar energy to thermal energy.[3]

Solar collectors are common devices for solar thermal conversion. Minardi and Chuang[4] first proposed the concept of direct absorption solar collector (DASC) in 1975. To improve the working performance of the collector, Choi[5] proposed the concept of applying nanofluid in a DASC. A Nanofluid is a suspension of nanoparticles with a diameter of no more than 100 nm in the base fluid. Water is the most common working base fluid.[6] By using nanofluids, the collector performance has been can be improved significantly.[7-11]

The absorption property of nanoparticles is critical in influencing the photothermal conversion performance of a DASC. The nanoparticle structure, size, and dielectric characteristics are the main factors determining the absorption properties of a nanoparticle.[12,13] Various nanofluids have been explored to realize better absorption.[14-18] Lee *et al.*[19] in 2012 proposed a kind of SiO_2/Au core-shell structure with local surface plasmon resonance (LSPR), and the thermal efficiency of direct absorption solar collector using these nanoparticles reaches 70%. In 2014, Zhang *et al.*[20] proposed to disperse Au nanoparticles into the base liquid, and the results showed that an Au nanofluid with a volume fraction of 0.015% could improve the photothermal conversion efficiency of the collector by 20%. It is worth mentioning that apart from metallic nanoparticles, carbon nanomaterials have also been

[1] *Korea Advanced Institute of Science and Technology, Daejeon 34141, South Korea.*
[2] *Institute of Thermal Science and Technology, Shandong University, Jinan 250061, China.*
[3] *College of Electromechanical Engineering, Qingdao University of Science and Technology, Qingdao 266061, China.*
[4] *Shandong Institute of Advanced Technology, Jinan 250100, China.*
**Email:* xiaohu.wu@iat.cn (X. Wu)

extensively investigated for solar energy harvest.[21-24] At the same time, various optimization schemes have been conducted to improve the performance of a DASC.[25-27]

However, due to the resonance nature of the absorption peak of LSPR, the absorption band of nanoparticles is severely limited in the narrow resonance band, leading to low energy absorption of solar radiation.[19,28] To achieve broadband absorption, Jeon *et al*.[29] tuned the resonance frequency of gold nanorods by adjusting the aspect ratio and successfully demonstrated the feasibility of broadband absorption by mixing a variety of gold nanorods in a fluid. Several new nanoparticles have been proposed to excite more absorption peaks to broaden the absorption band.[30-34] Besides LSPR, other resonance modes also exist such as magnetic polaritons,[35] hyperbolic modes,[36] surface phonon polaritons,[37] *etc*. The utilization of various resonance modes to broaden the absorption band has become a research hotspot. Recently, Qin *et al.*[38] have proposed an Ag-SiO_2-Ag nanodisk particle, and they have shown that the magnetic polaritons were excited besides LSPR, beneficial for broadband solar energy absorption.

However, the synthesis of the Ag-SiO_2-Ag nanodisk particles remains challenging. In this work, we proposed a core/shell/shell shape Ag-SiO_2-Ag composite nanoparticle considering the more feasible synthesis of core/shell nanoparticles.[39] The finite element method has been used to calculate the absorption properties of composite nanoparticles. The physical mechanisms for the absorption peaks have also been revealed. In addition, the effect of different sizes and materials on the absorption and scattering efficiencies has been investigated.

2. Modeling

Figure 1 shows the proposed Ag-SiO_2-Ag core/shell/shell shape composite nanoparticle. Silver is chosen in this work due to its small loss factor compared to other common metals.[40] The diameter of the inner silver core, the thickness of the middle silica layer, and the thickness of the outer silver layer are respectively d_1 = 20 nm, t_2 = 10 nm, and t_3 = 10 nm. These sizes are chosen to ensure that the absorption is significant while the scattering is not too strong for effective solar energy absorption.[41] The dimension remains unchanged in this study until further specified. The surrounding working fluid is water. The permittivity of silver, silica, and water is obtained in Ref.[42]. Only the visible wavelength range, *i.e.*, 300-800 nm, has been considered since the resonances induced by the nanoparticles usually fall in this range or at even shorter wavelengths.[41] The absorption and scattering efficiencies of the composite nanoparticles are evaluated with the finite element method by using the Wave Optics module in COMSOL Multiphysics. Owing to the symmetry of the nanoparticle, only one case of the light incidence is considered, *i.e.*, a plane wave incident towards the *x* direction and polarized along the *y* direction. The formulations based on Maxwell's equations and the material laws together predict the propagation of light in the media of different dielectric constants. A perfect matching layer (PML) with a thickness of 10 times the particle radius was also applied to envelop the nanoparticle so that the calculation space is truncated into a limited space without influencing the light propagation in the nanoparticle region, making the implementation of finite element method (FEM) calculation possible. For evaluating absorption efficiency and scattering efficiency, the obtained absorption cross-sections and scattering cross-sections need to be normalized by dividing the corresponding nanoparticle cross-sections.

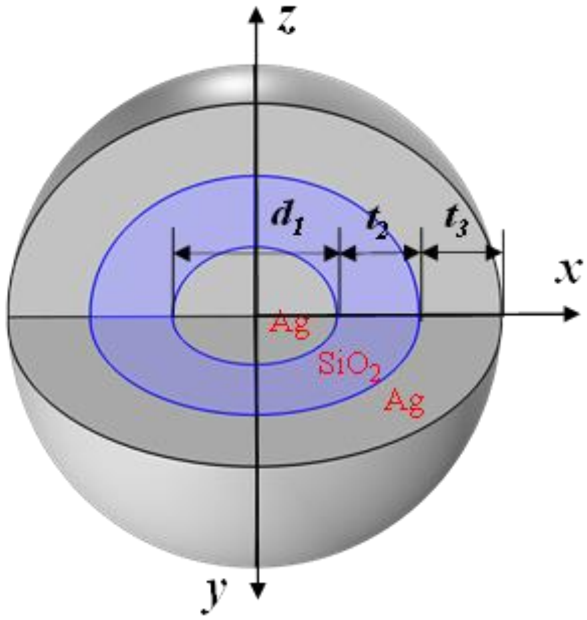

Fig. 1 Schematic of the proposed core/shell/shell shape Ag-SiO_2-Ag composite nanoparticle, with d_1 = 20 nm, t_2 = 10 nm, and t_3 = 10 nm.

3. Results and discussion

3.1 Absorption and scattering efficiencies

Figure 2(a) compares the absorption efficiency of the proposed Ag-SiO_2-Ag composite nanoparticle and a pure Ag nanoparticle with the same dimension (*i.e.* the radius of the Ag nanoparticle is 30 nm). It is seen that the Ag-SiO_2-Ag composite nanoparticle generates two distinct absorption peaks in the visible wavelength range. The main peak is at around 570 nm with an absorption efficiency of 5.8, while the second peak is at around 430 nm with an absorption efficiency of 1.2. The absorption efficiency of the Ag nanoparticle with a diameter of 60 nm is also plotted for comparison. One can see that the absorption peak of the Ag nanoparticle is also at around 430 nm with an absorption efficiency of 4.4. The composite nanoparticles can excite more absorption peaks, compared to pure silver nanoparticles. This difference lies in the fact that an isolated metallic nanoparticle is only capable to generate the localized surface plasmon resonance caused by collective resonance between the free electrons and the electric field of the incident light;[19,34] while in the case of Ag-SiO_2-Ag nanoparticle, additional magnetic resonance can be

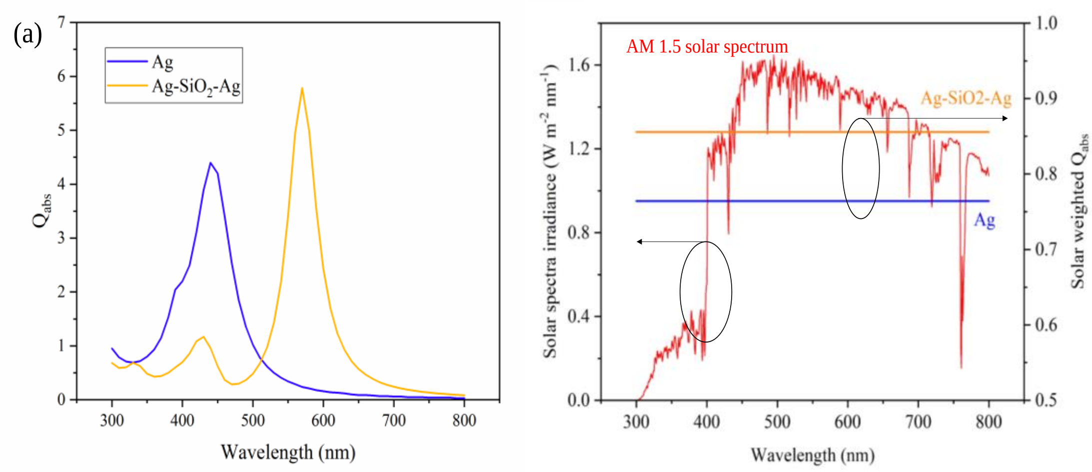

Fig. 2 Comparison of (a) absorption efficiency, (b) Solar weighted absorption efficiency of Ag and Ag-SiO_2-Ag [right axis], and the AM 1.5 solar spectral irradiance applied as the spectral weights [left axis].

excited due to the metal-insulator-metal structure, which is a typical morphology to excite magnetic resonance.[35,38]

In reality, the solar spectral irradiance is highly dependent on the wavelength, as shown in the red curve in Fig. 2(b). To take into account this wavelength dependency, the solar weighted absorption has been calculated. It turned out to be 0.855 and 0.764 for the Ag-SiO_2-Ag composite nanoparticle and the pure Ag nanoparticle, respectively. This implies an increase of about 10% for solar energy absorption by using the proposed Ag-SiO_2-Ag composite nanoparticle compared to the pure Ag nanoparticle.

3.2 Resonance mode analysis of the absorption peaks

Figure 2 has shown that the main peak and the secondary peak of Ag-SiO_2-Ag composite nanoparticles occur around 570 nm and 430 nm, respectively. To figure out the resonance modes of the absorption peaks, the local electric and magnetic fields at the resonance wavelengths are analyzed in this section.

The local electromagnetic field distribution in the nanoparticle at the wavelength of 570 nm is shown in Fig. 3, with Figs. 3(a) and (b) showing the *x*-*o*-*y* plane, Figs. 3(c) and (d) for the *x*-*o*-*z* plane. The electric and magnetic vectors are also shown to demonstrate their directions. In Fig. 3(a), it

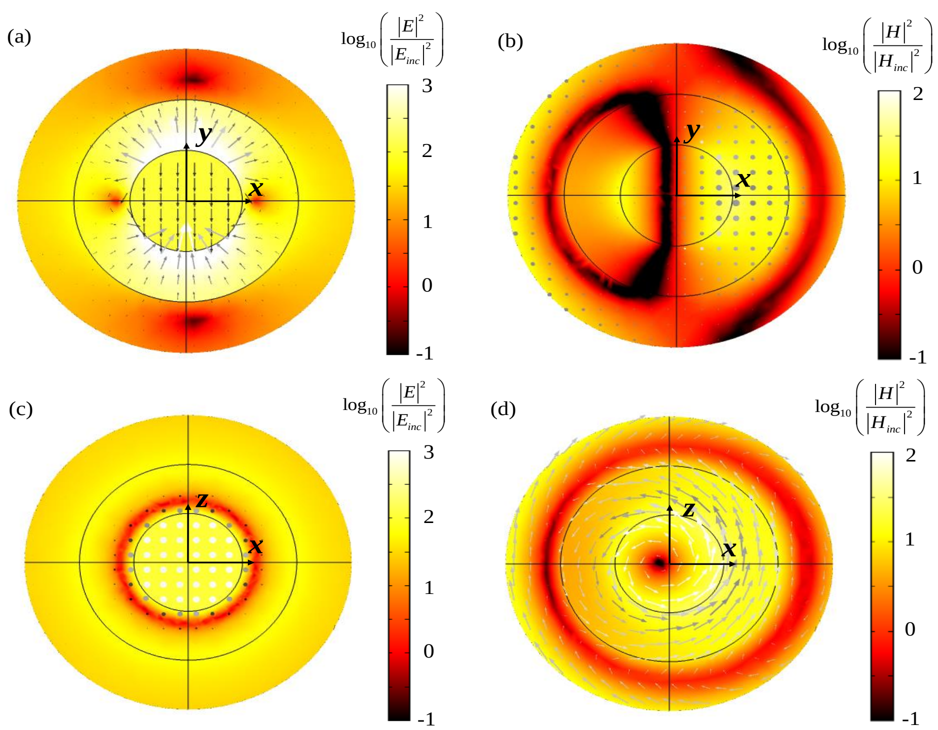

Fig. 3 Local field distribution at a wavelength of 570 nm for the Ag-SiO_2-Ag composite nanoparticle when the applied plane wave is *x*-incidence and *y*-polarization. Time-averaged square of (a) the electric field and (b) magnetic field distribution in the *x*-*o*-*y* plane; (c) the electric field and (d) magnetic field distribution in the *x*-*o*-*z* plane. The arrows denote the electric field vectors in Fig. 3(a), (c), and magnetic vectors in Fig. 3(b), (d) when the phase = 0 degrees.

is seen that the electric field intensity is symmetrically distributed along the x-axis and y-axis. The electric field intensity is relatively low in the inner Ag core and the outer Ag shell part, while magnified significantly in the middle SiO_2 shell, which is typical magnetic resonance characteristics.[35,38] The electric field intensity is especially high along the plane wave polarization direction (*i.e.* y direction) at the interface between the inner Ag core and the middle SiO_2 shell, and the maximum value can reach 54.6 V/m. Another interesting phenomenon is that a clockwise and an anti-clockwise circulate eddy current occurs respectively on the two sides near the interface between the Ag core and the SiO_2 middle shell along the plane wave incident direction (*i.e.* x direction). This verifies again the magnetic resonance at the wavelength of 570 nm. That is, the Ag core and the Ag outer shell work as the inductor while the SiO_2 inner shell works as a capacitor and they together form a resonant inductor-capacitor (LC) circuit and generate the anti-parallel eddy currents. As to the magnetic field distribution in Fig. 3(b), along the incident direction, the magnetic field presents a highly varying distribution. A relatively strong magnetic field is generated in a large region near the interface of the Ag core and the SiO_2 middle shell where $x > 0$, while localized in a small region where $x < 0$.

In the x-o-z plane, the electric field distribution as in Fig. 3(c) is centrally symmetrical, with a thin SiO_2 layer near the Ag core having lower electric field intensity, which corresponds to the two dark spots along the x-axis in Fig 3(a). From the magnetic field distribution as in Fig. 3(d), the strongest magnetic field is at the interface between the Ag core and the SiO_2 middle shell in the $x > 0$ side. The magnetic field gradually decreases both along $x > 0$ and $x < 0$. It is worth noting that a small area with the lowest magnetic field intensity occurs in the inner Ag core, and its center does not coincide with the center of the nanoparticle. The direction of the magnetic vectors (*i.e.* anti-clockwise here) indicates an opposite direction to that of the incidence plane wave (clockwise). This implies again that the resonance at 570 nm is attributed to magnetic resonance.

Now it comes to the absorption peak of the Ag-SiO_2-Ag composite nanoparticle near 430 nm as shown in Fig. 4. In the x-o-y plane in Fig. 4(a), the electric field is intensified largely at the interface between the Ag core and the middle SiO_2 shell along the polarization direction, and the electric vectors in the middle SiO_2 shell are consistently toward the polarization direction, indicating characteristics of LSPR. The peak near 430 nm also exists for the pure Ag nanosphere as in Fig. 2(a), and it is well known that individual silver nanoparticles cannot excite magnetic resonances, so the absorption peak near 430 nm is attributed to the excitation of electric resonance. The electric field distribution in the x-o-z plane in Fig. 4(b) shows clearly again that the electric field is intensified around the outer surface of the Ag core, which is a characteristic of the LSPR.

3.3 Tuning the optical properties of the Ag-SiO_2-Ag composite nanoparticle

Since the size of the nanoparticles has a significant effect on their optical properties, a parametric study was conducted to evaluate its impact. The sizes for d_1, t_2, and t_3. have been increased proportionally from 20, 10, and 10 nm until 40, 20, and 20 nm. The resulting absorption efficiency Q_{abs} of the Ag-SiO_2-Ag composite nanoparticles is shown in Fig. 5(a). It is observed that as d_1, t_2, and t_3 increase, a red shift occurs for the main peak near 570 nm, which is induced by magnetic resonance. The peak becomes broadened with a lower peak value. For the peak induced by LSPR near 430 nm, the peak value increases with the increase of the nanoparticle size, and a redshift also appears. The variation of the nanoparticle size can tune its absorption efficiency. A suitable combination of different sizes of nanoparticles in a nanofluid can thus reasonably achieve a broad absorption coefficient.[29,34] Besides absorption, scattering in a nanofluid also plays a significant role in determining the efficiency of solar energy harvest. Although scattering may cause a portion of the photons to be scattered out of the collector, it is not entirely

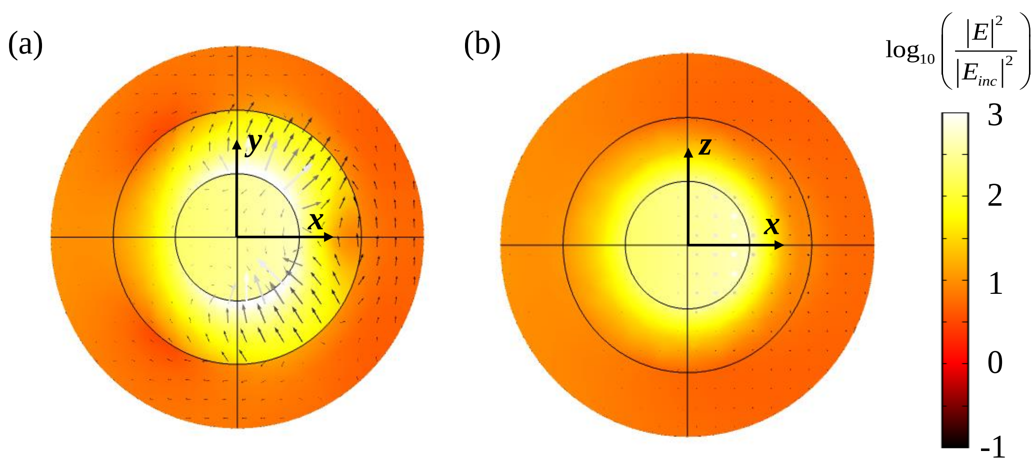

Fig. 4 Local field distribution at the wavelength of 430 nm for the Ag-SiO_2-Ag composite nanoparticle when the applied plane wave is x-incidence and y-polarization. The arrows indicate the electric field vector when the phase = 0 degrees.

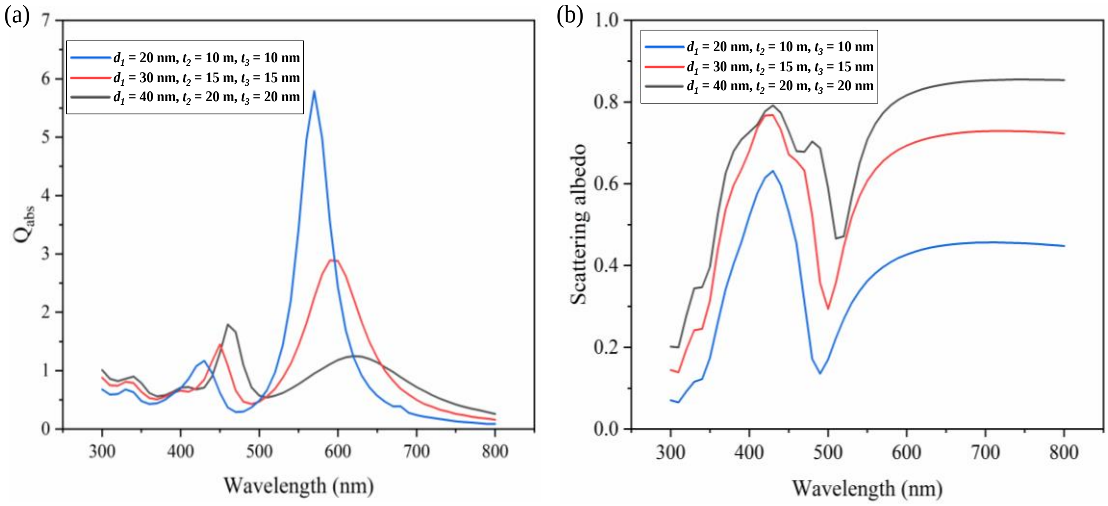

Fig. 5 Effects of nanoparticle sizes on (a) absorption efficiency and (b) scattering albedo of the Ag-SiO_2-Ag composite nanoparticle.

harmful because light scattering can increase the optical length of the photons. For instance, Won *et al.*[43] have theoretically evaluated the relation between the absorption efficiency and scattering efficiency and found that despite the absolute value of scattering efficiency, a carefully engineered scattering efficiency depending on the absorption efficiency can improve the collector performance. Therefore, it is necessary to control the scattering in a reasonable range, and wise choice and design of the nanoparticle size can contribute to the solar energy absorption further. The comparison of the corresponding scattering albedo, *i.e.* scattering efficiency/extinction efficiency, where extinction efficiency = (absorption efficiency + scattering efficiency), is shown in Fig. 5(b). It is seen that with the increase of the nanoparticle size, the scattering albedo keeps increasing, and this makes the tuning of the scattering efficiency feasible. Another interesting finding is that the scattering albedo at the magnetic resonance peak is much less compared to that at LSPR, which is beneficial for direct effective solar energy absorption. It is worth noting that the size parameters need not necessarily vary in proportion, *i.e.* one can change d_1, t_2, and t_3 separately as required.

Besides the size parameter, nanoparticle material also affects the optical properties significantly. Here, we compared the absorption efficiencies of the composite nanoparticles with several common metals, *i.e.* Ag, Cu, Zn, and Au. The real and imaginary parts of the complex refractive index, *n,* and *k*, which affect the optical properties of the nanoparticle, are shown in Fig. 6(a).[44] The resulting absorption efficiencies of the composite nanoparticles are in Fig. 6(b). It is obvious that the spectral absorption efficiency of the nanoparticles with different metal materials distinguishes them from each other. In the wavelength range of interest, the Ag-SiO_2-Ag nanoparticle has two distinct absorption peaks as discussed earlier. The Cu-SiO_2-Cu nanoparticle has one high peak of around 610 nm and a shoulder in the range of 300-550 nm with a relatively high absorption efficiency of 1.5. As to the Zn-SiO_2-Zn nanoparticle, only one broad peak occurs at around 450 nm, with a peak value of about 2. For the Au-SiO_2-Au nanoparticle, one main peak occurs near 650 nm, and a

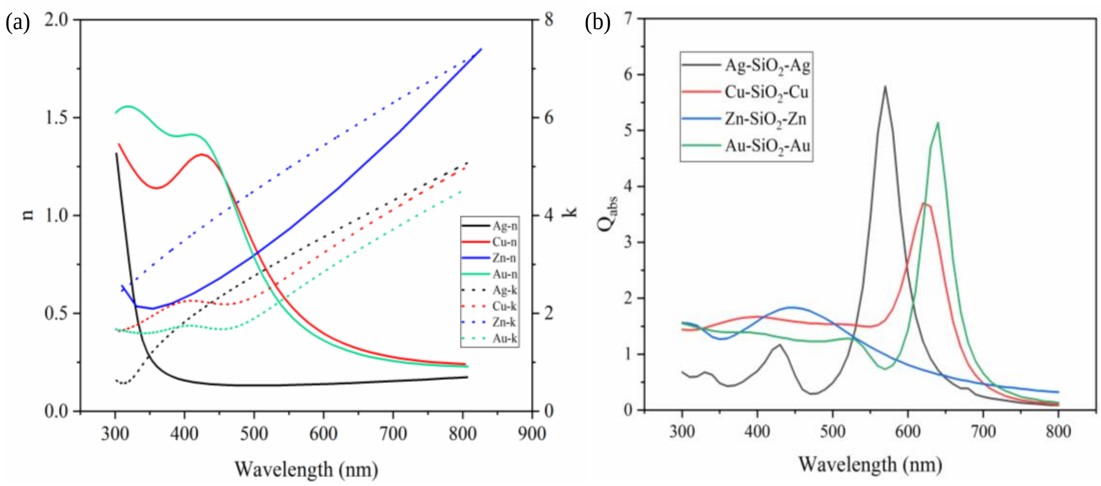

Fig. 6 (a) The real and imaginary parts of the complex refractive index, *i.e.*, *n* and *k* respectively, for the four metals, Ag, Cu, Zn, and Au.[44] (b) Effect of different metal materials on the absorption efficiency for the metal-insulator-metal composite nanoparticle. The sizes remain as d_1 = 20 nm, t_2 = 10 nm and t_3 = 10 nm.

wide shoulder with an absorption efficiency of around 1.3 exists in the range of 300-520 nm. The combination of nanoparticles of different materials is promising to realize broadband solar energy absorption. Further optimizations can be conducted to explore the optimized combination of the nanoparticles with different sizes and materials for optimum solar energy absorption.

4. Conclusion

In the work, the core/shell/shell shape metal-insulator-metal composite nanoparticles have been proposed for solar thermal harvest. The optical properties of the Ag-SiO_2-Ag composite nanoparticle have been evaluated, and multiple absorption peaks have been observed upon a plane wave incidence. The analysis of the distribution of the local electric and magnetic fields revealed that the absorption peaks were attributed to both the magnetic resonance and the electric resonance (*i.e.* LSPR). The size parametric study showed that the variation of the nanoparticle sizes can tune the peak magnitudes of the absorption peaks, as well as the corresponding scattering albedo. The change of materials is beneficial to obtain absorption peaks in different wavelengths. This work suggests that the core/shell/shell shape metal-insulator-metal composite nanoparticles can be promising candidates for efficient and broadband solar energy absorption.

Acknowledgment

The research was supported by the Shandong Provincial Natural Science Foundation (ZR2020LLZ004).

Conflict of interest

There are no conflicts to declare.

Supporting information

Not applicable.

References

[1] M. Chen, X. Chen, D. Wu, *Advances in Microfluidics and Nanofluids. IntechOpen*, 2021, doi: 10.5772/intechopen.96991.

[2] N. S. Lewis, *Science*, 2016, **351**, eaad1920, doi: 10.1126/science.aad1920.

[3] O. Mahian, E. Bellos, C. N. Markides, R. A. Taylor, A. Alagumalai, L. Yang, C. Qin, B. J. Lee, G. Ahmadi, M. R. Safaei, S. Wongwises, *Nano Energy*, 2021, **86**, 106069, doi: 10.1016/j.nanoen.2021.106069.

[4] J. E. Minardi, H. N. Chuang, *Solar Energy*, 1975, **17**, 179-183, doi: 10.1016/0038-092x(75)90057-2.

[5] Choi, S. US., Eastman, J. A., "Enhancing thermal conductivity of fluids with nanoparticles", *International mechanical engineering congress and exhibition (No. ANL/MSD/CP-84938; CONF-951135-29)*, 2015.

[6] H. Tyagi, P. Phelan, R. Prasher, *Journal of solar energy engineering*, 2009, **131**, 041004, doi: doi.org/10.1115/1.3197562.

[7] L. Zhang, J. Liu, G. He, Z. Ye, X. Fang, Z. Zhang, *Solar Energy Materials and Solar Cells*, 2014, **130**, 521-528, doi: 10.1016/j.solmat.2014.07.040.

[8] J. Jeon, S. Park, B. J. Lee, *Solar Energy*, 2016, **132**, 247-256, doi: 10.1016/j.solener.2016.03.022.

[9] C. Qin, J. Lee, B. J. Lee, *Applied Thermal Engineering*, 2021, **185**, 116333, doi: 10.1016/j.applthermaleng.2020.116333.

[10] H. Zhang, K. Wang, L. Wang, H. Xie, W. Yu, *Solar Energy*, 2020, **201**, 628-637, doi: 10.1016/j.solener.2020.03.047.

[11] D. Wang, Y. Fang, W. Yu, L. Wang, H. Xie, Y. Yue, *Solar Energy Materials and Solar Cells*, 2021, **220**, 110850, doi: 10.1016/j.solmat.2020.110850.

[12] X. Chen, P. Zhou, H. Yan, M. Chen, *Energy*, 2021, **216**, 119254, doi: 10.1016/j.energy.2020.119254.

[13] M. Chen, Y. He, J. Zhu, D. R. Kim, *Energy Conversion and Management*, 2016, **112**, 21-30, doi: 10.1016/j.enconman.2016.01.009.

[14] R. A. Taylor, P. E. Phelan, T. P. Otanicar, R. Adrian, R. Prasher, *Nanoscale Research Letters*, 2011, **6**, 225, doi: 10.1186/1556-276x-6-225.

[15] Y. Xuan, H. Duan, Q. Li, *RSC Advances*, 2014, **4**, 16206-16213, doi: 10.1039/c4ra00630e.

[16] Y. Wu, L. Zhou, X. Du, Y. Yang, *International Journal of Heat and Mass Transfer*, 2015, **82**, 545-554, doi: 10.1016/j.ijheatmasstransfer.2014.11.026.

[17] T. B. Gorji, A. A. Ranjbar, *Renewable and Sustainable Energy Reviews*, 2017, **72**, 10-32, doi: 10.1016/j.rser.2017.01.015.

[18] L. Wang, M. Wang, Z. Xu, W. Yu, H. Xie, *Solar Energy Materials and Solar Cells*, 2020, **212**, 110575, doi: 10.1016/j.solmat.2020.110575.

[19] B. J. Lee, K. Park, T. Walsh, L. Xu, *Journal of Solar Energy Engineering*, 2012, **134**, 021009, doi: 10.1115/1.4005756.

[20] H. Zhang, H.-J. Chen, X. Du, D. Wen, *Solar Energy*, 2014, **100**, 141-147, doi: 10.1016/j.solener.2013.12.004.

[21] J. Zeng, Y. Xuan, *Applied Energy*, 2018, **212**, 809-819, doi: 10.1016/j.apenergy.2017.12.083.

[22] V. Khullar, H. Tyagi, N. Hordy, T. Otanicar, Y. L. Hewakuruppu, P. Modi, R. A. Taylor, *International Journal of Heat and Mass Transfer*, 2014, **77**, 377384.

[23] N. Hordy, D. Rabilloud, J. L. Meunier, S. Coulombe, *Solar Energy*, 2014, **105**, 82-90, doi: 10.1016/j.solener.2014.03.013.

[24] T. Boldoo, M. Lee, H. Cho, *International Journal of Energy Research*, 2022, **46**, 8891-8907, doi: 10.1002/er.7763.

[25] C. Qin, K. Kang, I. Lee, B. J. Lee, *Solar Energy*, 2018, **169**, 231-236, doi: 10.1016/j.solener.2018.04.056.

[26] C. Qin, K. Kang, I. Lee, B. J. Lee, *Solar Energy*, 2017, **150**, 512-520, doi: 10.1016/j.solener.2017.05.007.

[27] J. Seo, C. Qin, J. Lee, B. J. Lee, *Scientific Reports*, 2020, **10**, 1-10, doi: 10.1038/s41598-020-65811-6.

[28] Z. Wang, X. Quan, Z. Zhang, P. Cheng, *Journal of Quantitative Spectroscopy and Radiative Transfer*, 2018, **205**, 291-298, doi: 10.1016/j.jqsrt.2017.08.001.

[29] J. Jeon, S. Park, B. J. Lee, *Optics Express*, 2014, **22**, A1101, doi: 10.1364/oe.22.0a1101.

[30] M. Chen, Y. He, J. Huang, J. Zhu, *Energy Conversion and Management*, 2016, **127**, 293-300, doi: 10.1016/j.enconman.2016.09.015.

[31] X. Liu, Y. Xuan, *Nanoscale*, 2017, **9**, 14854-14860, doi: 10.1039/c7nr03912c.
[32] X. Yu, Y. Xuan, *Solar Energy*, 2018, **160**, 200-207, doi: 10.1016/j.solener.2017.12.007.
[33] X. Wang, Y. He, M. Chen, Y. Hu, *Solar Energy Materials and Solar Cells*, 2018, **179**, 185-193, doi: 10.1016/j.solmat.2017.11.012.
[34] C. Qin, J. B. Kim, H. Gonome, B. J. Lee, *Renewable Energy*, 2020, **145**, 21-28, doi: 10.1016/j.renene.2019.05.133.
[35] B. Zhao, Z. M. Zhang, *Journal of Quantitative Spectroscopy and Radiative Transfer*, 2014, **135**, 81-89, doi: 10.1016/j.jqsrt.2013.11.016.
[36] A. Poddubny, I. Iorsh, P. Belov, Y. Kivshar, *Nature Photonics*, 2013, **7**, 948-957, doi: 10.1038/nphoton.2013.243.
[37] J. J. Greffet, R. Carminati, K. Joulain, J. P. Mulet, S. Mainguy, Y. Chen, *Nature*, 2002, **416**, 61-64, doi: 10.1038/416061a.
[38] C. Qin, Y. Guo, J. Seo, Y. Shuai, J. Lee, B. J. Lee, *Optics Express*, 2020, **28**, 15731, doi: 10.1364/oe.393351.
[39] R. Liu, R. D. Priestley, *Journal of Materials Chemistry A*, 2016, **4**, 6680-6692, doi: 10.1039/C5TA09607C.
[40] W. Cai, V. M. Shalaev, *Springer New York Dordrecht Heidelberg London*, 2010.
[41] C. F. Bohren, D. R. Huffman, *Wiley*, 1998, doi: 10.1002/9783527618156.
[42] E. D. Palik, *Amsterdam: Elsevier*, 1998, 691-703, doi: 10.1016/b978-0-08-055630-7.50042-0.
[43] K. H. Won, B. J. Lee, *Frontiers in Energy*, 2018, **12**, 169-177, doi: 10.1007/s11708-018-0527-5.
[44] Refractive index database, https://refractiveindex.info/ retrieved on July 1, 2021.

Author Information

Caiyan Qin *is currently a postdoctoral researcher in Korea Advanced Institute of Science and Technology (KAIST), South Korea. She received her Ph.D. degree from Department of Mechanical Engineering in KAIST in 2019, and Master's and Bachelor's Degree from School of Energy Science and Engineering in Harbin Institute of Technology, China in 2015 and 2012, respectively. Her research interests include solar energy applications, nanofluid utilization, plasmonics, as well as heat and mass transfer in MEMS devices.*

Xiaohu Wu *received his B.S. degree in engineering mechanics from China University of Mining and Technology (Beijing) and Ph. D. degree from Peking University under the guidance of Prof. Ceji Fu. He was a visiting student at Georgia Institute of Technology from Sept. 2017 to Sept. 2018 under the guidance of Prof. Zhuomin Zhang. Currently, Dr. Wu is an associate researcher at Shandong Institute of Advanced Technology. Dr. Wu's main research interest is on thermal radiative properties of anisotropic materials and applications. He has published about 60 peer-reviewed journal papers and given three conference presentations. His Ph.D. thesis was published by Springer Nature and was recognized as outstanding doctoral research. Dr. Wu is the winner (along with his advisors) of the 2019 Hartnett-Irvine Award by the International Centre for Heat and Mass Transfer. In addition, his work about hyperbolic materials was selected as "Optics in 2020" by Optics & Photonics News. Besides, two of his papers are selected as cover papers by ES Energy & Environment.*

